POSTBUCKLING EQUILIBRIUM PATH OF A LONG THIN-WALLED CYLINDRICAL SHELL (SINGLE-WALLED CARBON NANOTUBE) UNDER AXIAL COMPRESSION USING ENERGY METHOD

M. Mohammadimehr

Department of Mechanical Engineering, Shahid Bahonar University of Kerman, Kerman, Iran, mmohammadimehr@gmail.com

A. R. Saidi*

Department of Mechanical Engineering, Shahid Bahonar University of Kerman, Kerman, Iran, a_r_saidi@yahoo.com

A. Ghorbanpour Arani

Department of Mechanical Engineering, Faculty of Engineering, University of Kashan, Kashan, Iran, aghorban@kashanu.ac.ir

Q. Han

School of Civil Engineering and Transportation, South China University of Technology, Guangzhou, 510640, P. R. China, emqhan@scut.edu.cn

*Corresponding Author

(Received: February 25, 2009 – Accepted in Revised Form: March 11, 2010)

Abstract In this paper, an elastic shell model is presented for postbuckling prediction of a long thin-walled cylindrical shell under axial compression. The Ritz method is applied to solve the governing equilibrium equation of a cylindrical shell model based on the von-Karman type nonlinear differential equations. The postbuckling equilibrium path is obtained using the energy method for a long thin-walled cylindrical shell. Furthermore, the postbuckling relationship between the axial stress and end-shortening is investigated with different geometric parameters. Also, this theory is used for postbuckling analysis of a single-walled carbon nanotube without considering the small scale effects. Numerical results reveal that the single-walled carbon nanotube under axial compression has an unstable postbuckling behavior.

Keywords Postbuckling; Long Thin-Walled Shell; Axial Compression; Ritz Method; SWCNT

چکیده در این مقاله، مدل پوسته الاستیک برای پیش‌بینی مسیر بعد از کمانش پوسته استوانه‌ای جدار نازک طویل تحت فشار محوری ارائه می‌شود. روش ریتز برای حل کردن معادله حاکمه تعادل مدل پوسته استوانه‌ای براساس معادلات دیفرانسیل غیر خطی وان کارمن به کار برده می‌شود. مسیر بعد از کمانش برای پوسته استوانه-ای جدار نازک طویل با استفاده از روش انرژی به دست می‌آید. بعلاوه رابطه بعد از کمانش بین تنش محوری و کوتاه‌شدگی با پارامترهای هندسی مختلف بررسی می‌شود. همچنین این تئوری برای تحلیل رفتار پس از کمانش نانو لوله‌های کربنی تک جداره بدون در نظر گرفتن اثر مقیاس کوچک استفاده می‌شود. نتایج عددی نشان می‌دهد که نانو لوله کربنی تک جداره تحت فشار محوری بعد از کمانش رفتار ناپایداری دارد.

1. INTRODUCTION

Carbon nanotubes (CNTs) were discovered by Iijima in 1991 [1]. They are made of a highly ordered sheet of carbon atoms rolled into a tube form. This uniform structure gives CNTs their unique properties.

Many researchers investigated buckling of carbon nanotubes under axial compression and torsional loading, (see for example: Ru [2], Han and Lu [3], Zhang et al. [4], Sohi and Naghdabadi [5], Ranjbartoreh et al. [6] and Yao and Han [7])

but there are few works on postbuckling analysis of this materials in the literature.

Shen [8] presented an elastic double-shell model for the buckling and postbuckling of a double-walled carbon nanotube (DWCNT) subjected to external hydrostatic pressure. Yao and Han [9] investigated the buckling and postbuckling of a DWCNT under axial compression based on a continuum mechanics model. Shen and Zhang [10] presented thermal postbuckling analysis for a DWCNT subjected to combined axial and radial loads. Zhang and Han [11] considered buckling and postbuckling behaviors of imperfect cylindrical shell subjected to torsional moment. They obtained the governing equations based on the Karman-Donnell type nonlinear differential equations. In their work, the boundary layer theory used to obtain the solutions that meet the boundary conditions. Yao and Han [12] studied the governing equations for the buckling and postbuckling behavior based on the Karman-Donnell-type nonlinear differential equations. Yao et al. [13] investigated the bending buckling behaviors of single, double and multi-walled carbon nanotubes by using a modified finite element method (FEM).They examined the effects of the number of layers on the buckling load and critical bending angle of multi-walled carbon nanotubes. Moreover, they showed that their modified FEM is a fast and efficient way to study the buckling and postbuckling of CNTs.

In this paper, an elastic shell model is investigated for the postbuckling prediction of a long thin-walled cylindrical shell under axial compression. The Ritz method is applied to solve the governing equation based on the von-Karman type nonlinear differential equation for the large deflection. The postbuckling equilibrium path is obtained theoretically using the energy method for a long thin-walled cylindrical shell. Moreover, the postbuckling relationship between axial stress and end-shortening is presented with different geometric parameters. Also, this theory is used for postbuckling analysis of a single-walled carbon nanotube (SWCNT) without considering the small scale effects. Numerical results reveal that the SWCNT under axial compression has an unstable postbuckling behavior. The results are compared with both experimental and other theoretical results. The present method simply predicts the postbuckling behavior of CNTs.

2. THE ENERGY METHOD

Consider a cylindrical shell under axial compression P where E, ν, R and h represent the Young's modulus, Poisson's ratio, the middle radius and thickness of shell, respectively. Consider a Cartesian coordinate system with a center in the middle surface of the shell; x and y the axial and circumferential coordinates of the shell, respectively, and the z direction normal to the middle surface. Figure 1 shows a long thin-walled cylindrical shell with a Cartesian coordinate system. Also Figure 2 depicts a cylindrical shell element which the displacement components in the x, y and z directions has been defined as u, v and w, respectively.

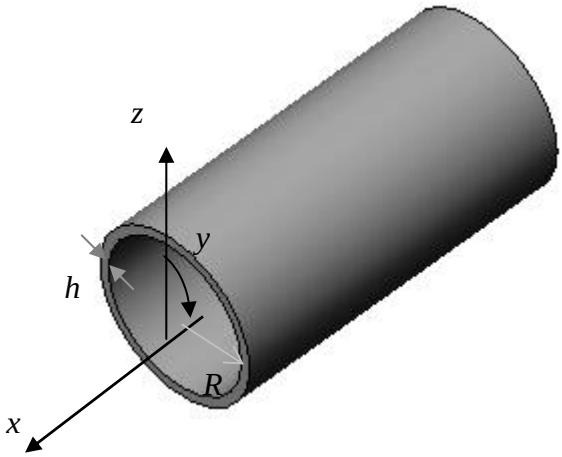

Figure 1. A long thin-walled cylindrical shell under axial compression.

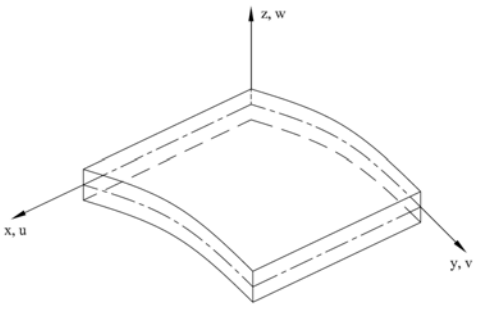

Figure 2. A cylindrical shell element.

According to Donnell type shell theory with von-Karman's large deflection assumptions, the relationships between strain and displacement components can be defined for a cylindrical shell as follows [14]

$$\begin{aligned}\varepsilon_x &= \bar{\varepsilon}_x + z\,k_x \\ \varepsilon_y &= \bar{\varepsilon}_y + z\,k_y \\ \gamma_{xy} &= \bar{\gamma}_{xy} + 2z\,k_{xy}\end{aligned} \tag{1}$$

where ε_x and ε_y are the normal strain in the x and y directions, respectively, and γ_{xy} represents the shear strain in the $x-y$ plane. Also $\bar{\varepsilon}_x$, $\bar{\varepsilon}_y$ and $\bar{\gamma}_{xy}$ are the nonlinear membrane strain components of the mid-plane and k_x, k_y and k_{xy} are the bending strain components which are defined as

$$\begin{aligned}\bar{\varepsilon}_x &= u_{,x} + \frac{1}{2}w_{,x}^{\,2} \\ \bar{\varepsilon}_y &= v_{,y} + \frac{w}{R} + \frac{1}{2}w_{,y}^{\,2} \\ \bar{\gamma}_{xy} &= u_{,y} + v_{,x} + w_{,x}\,w_{,y}\end{aligned} \tag{2}$$

$$\begin{aligned}k_x &= -w_{,xx} \\ k_y &= -w_{,yy} \\ k_{xy} &= -w_{,xy}\end{aligned} \tag{3}$$

The strain energy for an isotropic medium referred to arbitrary orthogonal coordinates may be written as

$$\begin{aligned}U &= \frac{1}{2}\iiint_V \sigma_{ij}\,\varepsilon_{ij}\,dV \\ &= \frac{1}{2}\iiint_V \left[\sigma_x\varepsilon_x + \sigma_y\varepsilon_y + \sigma_z\varepsilon_z + \sigma_{xy}2\varepsilon_{xy} + \sigma_{xz}2\varepsilon_{xz} + \sigma_{yz}2\varepsilon_{yz}\right]dx\,dy\,dz\end{aligned} \tag{4}$$

For plane stress state, the nonzero components of stress tensor are σ_x, σ_y and σ_{xy}. These stresses can be written in terms of the Airy's stress function $\varphi(x,y)$ as

$$\sigma_x = \frac{\partial^2\varphi}{\partial y^2}, \sigma_y = \frac{\partial^2\varphi}{\partial x^2}, \quad \sigma_{xy} = -\frac{\partial^2\varphi}{\partial x\,\partial y} \tag{5}$$

Substituting Eqs. (1)-(3) into Eq. (4) and applying relations (5), yields [15]

$$U_m = \frac{h}{2E}\iint_A \left[(\nabla^2\varphi)^2 - (1+\nu)\,L(\varphi,\varphi)\right]\,dx\,dy \tag{6}$$

and

$$U_b = \frac{D}{2}\iint_A \left[(\nabla^2 w)^2 - (1-\nu)\,L(w,w)\right]dx\,dy \tag{7}$$

where

$$\begin{aligned}\nabla^2 &= \frac{\partial^2}{\partial x^2} + \frac{\partial^2}{\partial y^2} \\ L(\chi_1,\chi_2) &= \frac{\partial^2\chi_1}{\partial x^2}\frac{\partial^2\chi_2}{\partial y^2} - \frac{\partial^2\chi_1}{\partial x\partial y}\frac{\partial^2\chi_2}{\partial x\partial y} + \frac{\partial^2\chi_1}{\partial y^2}\frac{\partial^2\chi_2}{\partial x^2}\end{aligned} \tag{8}$$

U_m and U_b denote the membrane and the bending strain energy of the shell, respectively.
Using Eq. (5), the stress function $\varphi(x,y)$ has to meet the compatibility equation as follows [15]:

$$\frac{1}{E}\nabla^4\varphi + \frac{1}{R}\frac{\partial^2 w}{\partial x^2} = -\frac{1}{2}L(w,w) \tag{9}$$

3. THE GOVERNING EQUATIONS FOR POSTBUCKLING OF A SWCNT UNDER AXIAL COMPRESSION

The Ritz method is applied to solve the governing equation (9) based on von Karman nonlinear type differential equation. Consider the deflection w as [15]

$$w(x,y) = f_0 + f_1\sin(\alpha x)\sin(\beta y) + f_2\left[\sin(\alpha x)\sin(\beta y)\right]^2 \tag{10}$$

where $\alpha = \frac{m\pi}{L}$, $\beta = \frac{n}{R}$.

and m and n are also axial and circumferential wave numbers. Substituting Eq. (10) into Eq. (9), one can find the following equation:

$$\frac{1}{E}\nabla^4\varphi = \frac{\alpha^2\beta^2}{2}(f_1^{\,2} + f_2^{\,2})(\cos 2\alpha x + \cos 2\beta y) - \frac{\alpha^2\beta^2}{2} f_2^{\,2}(\cos 4\alpha x + \cos 4\beta y) - \frac{\alpha^2}{R} f_2 \cos 2\alpha x + \alpha^2 f_1(\frac{1}{R} - \beta^2 f_2)\sin\alpha x \sin\beta y + \alpha^2 f_2(\frac{1}{R} - \beta^2 f_2)\cos 2\alpha x \cos 2\beta y + \frac{\alpha^2\beta^2}{2} f_2^{\,2}(\cos 4\alpha x \cos 2\beta y + \cos 2\alpha x \cos 4\beta y) + \frac{3}{2}\alpha^2\beta^2 f_1 f_2(\sin 3\alpha x \sin\beta y + \sin\alpha x \sin 3\beta y) \quad (11)$$

The solution of the partial differential equation (11) yields

$$\frac{1}{E}\varphi = g_1\cos 2\alpha x + g_2\cos 2\beta y + g_3\cos 4\alpha x + g_4\cos 4\beta y + g_5\sin\alpha x\sin\beta y + g_6\cos 2\alpha x\cos 2\beta y + g_7\cos 4\alpha x\cos 2\beta y + g_8\cos 2\alpha x\cos 4\beta y + g_9\sin 3\alpha x\sin\beta y + g_{10}\sin\alpha x\sin 3\beta y - \frac{P}{E}\frac{y^2}{2} \quad (12)$$

The constants $g_1 - g_{10}$ are shown in Appendix A.

Using Eqs. (6) and (12), the membrane strain energy of the shell can be obtained as

$$U_m = \frac{\pi}{2}hRLE\{g_1^{\,2}(2\alpha)^4 + g_2^{\,2}(2\beta)^4 + g_3^{\,2}(4\alpha)^4 + g_4^{\,2}(4\beta)^4 + \frac{1}{2}g_5^{\,2}(\alpha^2+\beta^2)^2 + \frac{1}{2}g_6^{\,2}(4\alpha^2+4\beta^2)^2 + \frac{1}{2}g_7^{\,2}(16\alpha^2+4\beta^2)^2 + \frac{1}{2}g_8^{\,2}(4\alpha^2+16\beta^2)^2 + \frac{1}{2}g_9^{\,2}(9\alpha^2+\beta^2)^2 + \frac{1}{2}g_{10}^{\,2}(\alpha^2+9\beta^2)^2 + 2\frac{P^2}{E^2}\} \quad (13)$$

Substituting Eq. (10) into Eq. (7), the bending strain energy of the shell can be written as

$$U_b = \frac{D}{2}\pi RL\{\frac{1}{2}f_1^{\,2}\alpha^4 + \frac{3}{2}f_2^{\,2}\alpha^4 + \frac{1}{2}f_1^{\,2}\beta^4 + \frac{3}{2}f_2^{\,2}\beta^4 + \alpha^2\beta^2(f_1^{\,2}+f_2^{\,2})\} \quad (14)$$

where $D = \frac{Eh^3}{12(1-\nu^2)}$.

The end-shortening relationship of the tube is defined as

$$e = \frac{1}{2\pi RL}\int_0^{2\pi R}\int_0^{L}\frac{\partial u}{\partial x}dx\,dy = \frac{1}{2\pi RL}\int_0^{2\pi R}\int_0^{L}\left[\frac{1}{E}(\frac{\partial^2\varphi}{\partial y^2} - \nu\frac{\partial^2\varphi}{\partial x^2}) - \frac{1}{2}(\frac{\partial w}{\partial x})^2\right]dx\,dy \quad (15)$$

where $e = \frac{\Delta x}{L}$. The potential energy of the external loads V, can be written as:

$$V = -\frac{Ph}{E}\int_0^{2\pi R}\int_0^{L}\left[\frac{\partial^2\varphi}{\partial y^2} - \nu\frac{\partial^2\varphi}{\partial x^2} - \frac{E}{2}(\frac{\partial w}{\partial x})^2\right]dx\,dy = \frac{2Ph}{E}\pi RL\left[P + \frac{\alpha^2 E}{8}(f_1^{\,2} + \frac{3}{4}f_2^{\,2})\right] \quad (16)$$

The total potential energy Π is

$$\Pi = U + V \quad (17)$$

From the variational calculus, the following relation can easily be written as:

$$\delta\Pi = \frac{\partial\Pi}{\partial f_1}\delta f_1 + \frac{\partial\Pi}{\partial f_2}\delta f_2 = 0 \quad (18)$$

It is convenient to define the following dimensionless quantities

$$\zeta = \frac{f_1}{h},\ \ \psi = \frac{f_2}{f_1} = \frac{\xi}{\zeta},\ \ \xi = \frac{f_2}{h},\ \ \overline{P} = \frac{P}{E}\frac{R}{h},\ \ \theta = \frac{\alpha}{\beta},\ \ \eta = \beta^2 hR,\ \ \overline{e} = e\frac{R}{h},\ \ \lambda_p = \frac{\sigma_x}{\sigma_{cr}},\ \ \delta_p = \frac{E}{\sigma_{cr}}e,\ \ \overline{Z} = \frac{L^2}{Rh} \quad (19)$$

Partial differentiation of Π with respect to f_1 and f_2 variables yield:

$$\overline{P} = B_1 + B_2\zeta^2 + B_3\psi^2\zeta^2 + B_4\psi\zeta \quad (20\text{-a})$$

$$B_5\psi^3\zeta^2 + B_6\psi^2\zeta + (B_7 + B_8\zeta^2)\psi + B_9\zeta = 0 \quad (20\text{-b})$$

The constants $B_1 - B_9$ are shown in Appendix B.

Applying Eqs. (19) on Eq. (20-b), it can be obtained

$$\zeta^2 = -\frac{B_5\xi^3 + B_6\xi^2 + B_7\xi}{B_8\xi + B_9} \tag{21}$$

Substituting Eq. (21) into Eq. (20-a), yields the following equation for nondimensional axial compression, $\overline{P}$

$$\overline{P} = B_1 - B_2\frac{B_5\xi^3 + B_6\xi^2 + B_7\xi}{B_8\xi + B_9} + B_3\xi^2 + B_4\xi \tag{22}$$

Applying the dimensionless quantities, and substituting Eqs. (10) and (12) into Eq. (15), $\overline{P}$ can be simplified as

$$\overline{P} = \overline{e} - \frac{1}{32}\eta\theta^2(-4\frac{B_5\xi^3 + B_6\xi^2 + B_7\xi}{B_8\xi + B_9} + 3\xi^2) \tag{23}$$

4. NUMERICAL RESULTS

Yamaki [16] reported precise experimental results on the postbuckling behavior of cylindrical shell under compression. To make a distinct comparison with his experimental results, the calculations are carried out for the same case by considering $\nu = 0.3$, $R/h = 405$ and $\overline{Z} = 210$ [17,18].

Figure 3 illustrates the dimensionless buckling load of a long thin-walled cylindrical shell versus axial end-shortening. It can be seen that the present model yields closer results to the experimental results (Yamaki [16]) than the results reported by Shen [17] for various wave numbers in the circumferential direction (n). Furthermore, the postbuckling paths contain the wide region for the large aspect ratio (L/R). It is noted that the effect of imperfection is not concluded in the present study and the differences in the curves should be attributed to the initial imperfections.

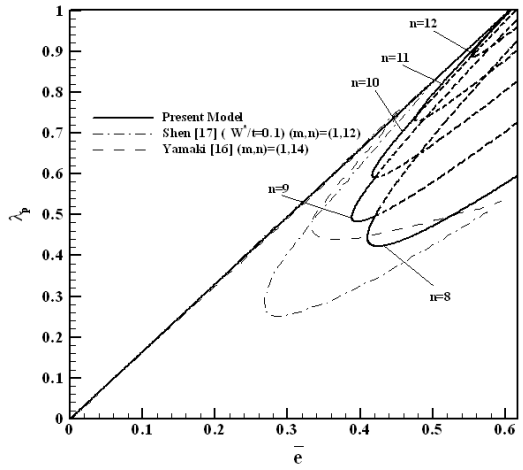

Figure 3. Comparing the analytical and experimental results.

Figure 4 shows the postbuckling path of a long thin-walled cylindrical shell under axial compression. The results are also compared with those obtained by Shen [18]. It can be seen that the present model predicts the postbuckling path very well.

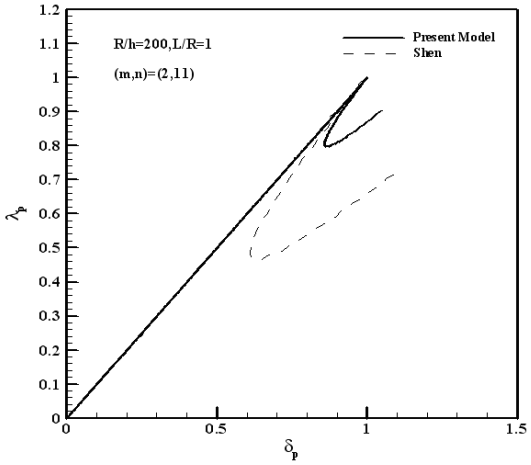

Figure 4. Postbuckling behavior of the cylindrical shell.

As an approximation, let us apply the presented method to the postbuckling analysis of a single walled carbon nanotube (SWCNT). In this analysis, the small scale effect is ignored. Also, for a SWCNT the van der Waals force is vanished. The material properties are assumed to be [19]

$$E = 5.5Tpa,\ t = 0.066nm,\ \nu = 0.19$$
$$D = 0.85\,eV(1eV = 1.6\times10^{-19}\,N.m),\ Et = 360J/m^2 \tag{24}$$

Figure 5 gives the postbuckling path for SWCNTs with different values of R/h. The aspect ratio (L/R) is considered to be 10. It is noted that for various values of R/h, the axial and circumferential buckling mode numbers (m,n) are different. The results show that the load-shortening curve is nonlinear and for a SWCNT, the decrease in loading generally goes with the increase in deformation in the initial postbuckling region and the postbuckling equilibrium path is unstable.

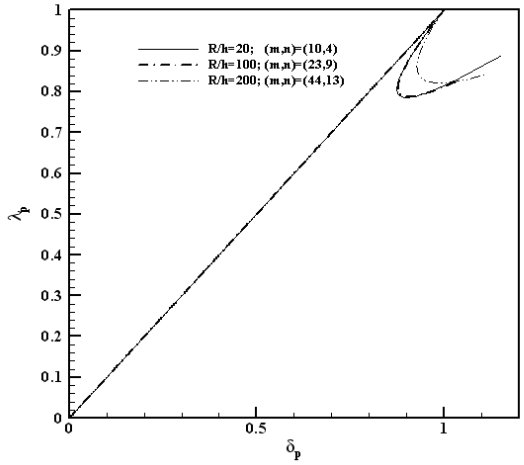

Figure 5. Postbuckling behavior of the carbon nanotubes with various radius to thickness ratios, $L/R=10$.

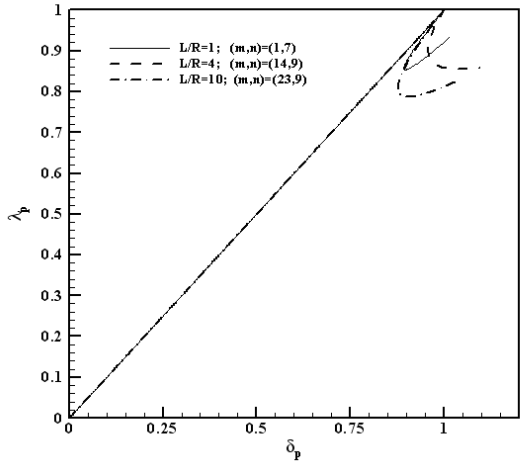

Figure 6. Postbuckling behavior of the carbon nanotubes with various aspect ratios, $R/h=100$.

Figure 6 shows the postbuckling behavior of a SWCNT under axial compression with different aspect ratios and $R/h=100$. It can be seen that the load-shortening curve is nonlinear and the postbuckling behavior includes the wide region for large aspect ratios. The results show that the postbuckling equilibrium path is unstable for SWCNTs.

5. CONCLUSIONS

In this work, an elastic shell model has been presented for the postbuckling prediction of a long thin-walled cylindrical shell under axial compression. The Ritz method was applied to solve the governing equation based on the von-Karman type nonlinear differential equations for large deflection. Also, the postbuckling equilibrium path was obtained theoretically using the energy method for a long thin-walled cylindrical shell. Moreover, the postbuckling relationship between axial stress and end-shortening has been investigated with different geometrical parameters. Also, this theory was used for postbuckling analysis of a single-walled carbon nanotube without considering the small scale effects. Numerical results reveal that the single-walled carbon nanotube under axial compression had an unstable postbuckling behavior. It was observed that the decrease in loading generally was accompanied by the increase in deformation in the initial postbuckling region and the postbuckling equilibrium region was greater for the thin nanotubes. It was found that the present model yields closer results to the experimental results (obtained by Yamaki [16]) comparing with the results reported by Shen [17] for various wave numbers in the circumferential direction. Furthermore, the postbuckling behavior contains the wide region for the large aspect ratios. The present model can simply predict the postbuckling behavior of SWCNTs.

To find more accurate results for postbuckling analysis of a single-walled carbon nanotube, the small scale and elastic medium effects should be considered in the further works. Also this method can be used for postbuckling analysis of double walled carbon nanotubes by considering the the van der Waals forces between the inner and outer nanotubes.

6. ACKNOWLEDGEMENTS

The authors wish to thank the referees for their valuable comments. The authors would like to acknowledge the Iranian Nanotechnology Development Committee for their financial support. The fourth author also gratefully acknowledges the supports from the National Natural Science Foundation of China (10672059) and the Natural Science Foundation of Guangdong Province (06025689).

APPENDIX A

The constants g_1-g_{10} in Eqs. (12) are as follows

$$g_1 = \frac{1}{16\alpha^2}\left(\frac{\beta^2 f_1^{\,2}}{2} + \frac{\beta^2 f_2^{\,2}}{2} - \frac{f_2}{R}\right)$$

$$g_2 = \frac{\alpha^2}{32\beta^2}\left(f_1^{\,2} + f_2^{\,2}\right)$$

$$g_3 = -\frac{\beta^2}{512\alpha^2} f_2^{\,2}$$

$$g_4 = -\frac{\alpha^2}{512\beta^2} f_2^{\,2}$$

$$g_5 = \frac{\alpha^2}{(\alpha^2+\beta^2)^2} f_1\left(\frac{1}{R} - \beta^2 f_2\right)$$

$$g_6 = \frac{\alpha^2}{(4\alpha^2+4\beta^2)^2} f_2\left(\frac{1}{R} - \beta^2 f_2\right)$$

$$g_7 = \frac{\alpha^2\beta^2 f_2^{\,2}}{2(16\alpha^2+4\beta^2)^2}$$

$$g_8 = \frac{\alpha^2\beta^2 f_2^{\,2}}{2(4\alpha^2+16\beta^2)^2}$$

$$g_9 = \frac{3\alpha^2\beta^2}{2(9\alpha^2+\beta^2)^2} f_1 f_2$$

$$g_{10} = \frac{3\alpha^2\beta^2}{2(\alpha^2+9\beta^2)^2} f_1 f_2$$

APPENDIX B

The constants $B_1 - B_9$ in Eqs. (20) are as follows

$$B_1 = \frac{(1+\theta^2)^2}{12(1-\nu^2)\theta^2}\eta + \frac{\theta^2}{\eta(1+\theta^2)^2}$$

$$B_2 = \frac{1+\theta^4}{16\theta^2}\eta$$

$$B_3 = \frac{\eta}{16\theta^2}\left[1+\theta^4 + \frac{16\theta^4}{(1+\theta^2)^2} + \frac{36\theta^4}{(1+9\theta^2)^2} + \frac{36\theta^4}{(9+\theta^2)^2}\right]$$

$$B_4 = -\frac{1}{8\theta^2}\left[1 + \frac{16\theta^4}{(1+\theta^2)^2}\right]$$

$$B_5 = \frac{5}{192}\left[1+\theta^4 + \frac{8\theta^4}{5(1+4\theta^2)^2} + \frac{8\theta^4}{5(4+\theta^2)^2} - \frac{32\theta^4}{(1+\theta^2)^2} - \frac{432\theta^4}{5(1+9\theta^2)^2} - \frac{432\theta^4}{5(9+\theta^2)^2}\right]$$

$$B_6 = -\frac{1}{8\eta}\left[1 - \frac{14\theta^4}{(1+\theta^2)^2}\right]$$

$$B_7 = \frac{9(1+\theta^4)+2\theta^2}{36(1-\nu^2)} + \frac{1}{6}\left[1 - \frac{11\theta^4}{2(1+\theta^2)^2}\right]\frac{1}{\eta^2}$$

$$B_8 = \frac{1}{48}\left[1+\theta^4 + \frac{64\theta^4}{(1+\theta^2)^2} + \frac{144\theta^4}{(1+9\theta^2)^2} + \frac{144\theta^4}{(9+\theta^2)^2}\right]$$

$$B_9 = -\frac{1}{12\eta}\left[1 + \frac{16\theta^4}{(1+\theta^2)^2}\right]$$

7. REFERENCES

1. Iijima, S., "Helical micro tubes of graphitic carbon", ***Nature***, Vol. 354, (1991), 56-58.
2. Ru, C. Q., "Axially compressed buckling of a double-walled carbon nanotube embedded in an elastic medium", ***Journal of the Mechanics and Physics of Solids***, Vol. 49, (2001), 1265-1279.
3. Han, Q. and Lu, G., "Torsional buckling of a double-walled carbon nanotube embedded in an elastic medium", ***European Journal of Mechanics A/Solids***, Vol. 22, (2003), 875-883.
4. Zhang, Y. Q., Liu, G. R., Qiang, H. F. and Li, G. Y., "Investigation of buckling of double-walled carbon nanotube embedded in an elastic medium using the energy method", ***International Journal of Mechanical Sciences***, Vol. 48, (2006), 53-61.
5. Sohi, A. N. and Naghdabadi, R., "Torsional buckling of carbon nanopeapods", ***Carbon***, Vol. 45, (2007), 952-957.
6. Ranjbartoreh, A. R., Ghorbanpour, A. and Soltani, B., "Double-walled carbon nanotube with surrounding elastic medium under axial pressure", ***Physica E***, Vol. 39, (2007), 230-239.

7. Yao, X. and Han, Q., "Investigation of axially compressed buckling of a multi-walled carbon nanotube under temperature field", ***Composites Science and Technology***, Vol. 67, (2007), 125-134.
8. Shen, H. S., "Postbuckling prediction of double-walled carbon nanotubes under hydrostatic pressure", ***International Journal of Solids and Structures***, Vol. 41, (2004), 2643-2657.
9. Yao, X. and Han, Q., "Postbuckling prediction of double-walled carbon nanotubes under axial compression", ***European Journal of Mechanics A/Solids*** , Vol. 26, (2007), 20-32.
10. Shen, H. S. and Zhang, C. L., "Postbuckling of double-walled carbon nanotubes with temperature dependent properties and initial defects under combined axial and radial mechanical loads", ***International Journal of Solids and Structures***, Vol. 44, (2007), 1461-1487.
11. Zhang, X. and Han, Q., "Buckling and postbuckling behaviors of imperfect cylindrical shells subjected to torsion", ***Thin-walled Structures***, Vol. 45, (2007), 1035-1043.
12. Yao, X. and Han, Q., "Torsional buckling and postbuckling equilibrium path of double-walled carbon nanotubes", ***Composites Science and Technology***, Vol. 68, (2008), 113-120.
13. Yao, X., Han, Q., and Xin, H., "Bending buckling behaviors of single- and multi-walled carbon nanotubes", ***Computational Materials Science***, Vol. 43, (2008), 579-590.
14. Brush, D. O. and Almroth, B. O., "Buckling of bars, plates and shells", ***McGraw-Hill***, (1975), New York.
15. Wu, L.Y., "Theory of plates and shells", ***Shanghai Jiaotong University Press***, (1989), Shanghai [in Chinese].
16. Yamaki, N., "Postbuckling and imperfection sensitivity of circular cylindrical shells under compression", In: Koiter WT, editor. ***Theoretical and applied mechanics. Horth-Holland Publishing Company***, (1976), 461-487.
17. Shen, H. S., "Postbuckling analysis of axially-loaded functionally graded cylindrical shells in thermal environments", ***Composites Science and Technology***, Vol. 62, (2002), 977-987.
18. Shen, H. S., "Postbuckling behavior of plates and shells", ***China: Science and Technology Press***, (2002), Shanghai [in Chinese].
19. Yakobson, B. I., Brabec, C. J. and Bernholc, J., "Nanomechanics of Carbon Tubes: Instabilities beyond Linear Response", ***Physical Review Letters***, Vol. 76, (1996), 2511-2514.